

# Various Thermal Coefficients Investigation of 3C-SiC Nanoparticles at the Different Heating Rates

Elchin Huseynov (✉ [elchin.h@yahoo.com](mailto:elchin.h@yahoo.com))

Azerbaijan National Academy of Sciences Institute of Radiation Problems <https://orcid.org/0000-0003-4202-7319>

Tural G. Naghiyev

Azerbaijan State Economic University: Azerbaijan State University of Economics

---

## Research Article

**Keywords:** nanocrystalline 3C-SiC, nanomaterials, thermal parameters

**Posted Date:** April 14th, 2021

**DOI:** <https://doi.org/10.21203/rs.3.rs-416201/v1>

**License:** © ⓘ This work is licensed under a Creative Commons Attribution 4.0 International License.

[Read Full License](#)

---

# Abstract

Several thermal parameters were analyzed for nanocrystalline silicon carbide (3C-SiC) particles at the performed depending on the thermal processing rate. The hydroxyl groups on the surface of nanocrystalline 3C-SiC particles have been investigated as a function of temperature and heating rate. Specific heat capacity and Gibbs energy of silicon carbide nanoparticles have been determined in the temperature range of 300 ÷ 1270K at the various heating rates. The enthalpy and the entropy were calculated at different thermal processing rates (theoretical calculations are confirmed based on experimental results). Experimental results obtained for all thermophysical parameters were comparatively studied at different thermal processing rates.

**PACS:** 61.46.+w, 65.80.+n, 67.80.Gb

## 1. Introduction

Over the past few years, various modifications of silicon carbide are widely used at modern technological devices in different directions [1–3]. Silicon carbide has a various polytypes or modifications and the most widely used of which are cubic (3C-SiC) and hexagonal (4H-SiC or 6H-SiC) silicon carbide compounds. The superiority of the physical properties of these compounds and their resistance to high temperatures have led to the expansion of their application fields [4–7]. Silicon carbide is an extremely significant material in devices and equipments used at high temperatures. Therefore, the study of thermal resistance of these types of compounds is very important and interesting.

Nanomaterials are characterized a high specific surface area (Specific Surface Area - SSA) and therefore have different physical properties than bulk materials. In this regard, as with other nano-sized materials, silicon carbide also has unique functional physical properties in nanoscales [8–11]. Considering these properties, we are also widely investigated silicon based nanomaterials under the influence of ionizing radiation [12–25]. Simultaneously, transmutation reaction, computational modeling, and gamma irradiation effects on such type nanomaterial investigated in various papers [26–29]. It should be note that there are distinct difference in the heat processes on th surface, various physical properties, in particular, thermophysical properties of the materials.

Unlike classic thermodynamics the new states are observed in nano sizes, and this cause to origin new interdisciplinary nanothermodynamic theory [30–33]. Several models of nanothermodynamic theory are known since today, which this theory play a connection role between macroscopic and nanoscopic theories. Recently, the nanothermodynamic theory is extensively used to investigated size dependence of the thermophysical properties of nanomaterials. In the presented work, the thermal processes occurring on the surface of nanocrystalline 3C-SiC particles have been studied with different heating rates. Specific heat capacity, free Gibbs energy, enthalpy and entropy of the nanocrystalline 3C-SiC particles have been investigated at the various heating rate.

## 2. Experiment

Cubic modification nanocrystalline 3C-SiC particles (Manufacturer: US Research Nanomaterials, Inc., TX, USA) were taken as a research object with 18 nm particle size, 120 m<sup>2</sup>/g specific surface area (SSA), 0.03 g/cm<sup>3</sup> density in nano scale (real density is 3.216 g/sm<sup>3</sup>) and 99+% purity. The measurements were carried out at "Perkin Elmer" STA 6000 equipment. Operating temperature range was from 290K to 1273 K, thermal processing rate 5, 10, 15 and 20 K/min, PolyScience analyzer and "digital temperature controller" were cooling system. Kinetic parameters were determined using "Pyris Manager" software. Argon inert gas is used and supplied to the system at a rate of 20 ml/min in order to remove the combustion products from the system and prevent the condensation process. Standard aluminum oxide based container (177,78 mg) was used in the experiments. An electronic recording device placed on the thermocouple determines the mass of the sample with an accuracy of 10<sup>-6</sup> g and records it automatically. The software automatically determines the difference between the mass of the sample-filled and empty container. Specified mass is stored in the software. The parameters of endo and exothermic effects in thermal spectra are calculated using the "Calculation" menu. All the results obtained in the experiments and in accordance with the theoretically calculated values are graphically described in the program "OriginPro 9.0".

## 3. Results And Discussion

In the general approach, the thermal parameters of nanocrystalline 3C-SiC particles have been studied to some extent. However, the physical processes on the surface of the 3C-SiC nanocrystals have not explained in the previous studies [12, 13]. The study of surface processes, the effect of temperature on such processes and the adsorption cases from the atmosphere are extremely relevant in the use of materials [34–39]. It is important to note that nanocrystalline 3C-SiC particles has a very large specific surface area (120 m<sup>2</sup>•g<sup>-1</sup>) like other nanomaterials. This causes to extremely active surface of the nanocrystalline 3C-SiC particles. As a result, 3C-SiC nanocrystals adsorb water molecules with high sensitivity when in contact with the atmosphere, causing the formation of O and H groups on the surface. The analysis showed that the hydroxyl or OH groups formed on the surface are not sufficiently stable at relatively high temperatures. Thus, as shown in Fig. 1, the OH groups begin to leave the surface of the nanomaterial depending on the heating rate, starting from the temperature values of about 467-483K. This process ends at a temperature of about 740-755K, and the energy supplied to the system is used to increase the Gibbs energy, entropy, and enthalpy (Figs. 2, 3, and 4). It is important to note that, heating rate directly affected to the hydroxyl groups dispersion time on the surface and temperature range of dispersion of OH radicals which is collected on the surface of 3C-SiC nanocrystals. Therefore, if this process occurs in the temperature range of 467-740K by low heating rate (5K/min), there is a shift in this process at relatively high heating rate (20K/min), and OH groups leave the nanomaterial in the temperature range 483-755K.

The temperature may increase with a constant rate or with some fluctuations during thermal analysis depending on the state of the system. Although the software of the devices provides a constant rate of thermal processing in real experiments, there are more or less fluctuations observed in the increasing of temperature. In this case, there is a very small difference in the temperature of the sample and the program of device, as well as other physical parameters [12, 40]. We can calculate the specific heat capacity of the system according to the heat flow if consider that  $dQ = C_p dT$  in the classical approach [12, 13, 40, 41]:

$$c_p = \frac{C_p}{m} = \frac{\frac{dQ_s}{dt}}{m \cdot \frac{dT}{dt}} = \frac{\Phi_s}{m \cdot \beta} = \frac{\Phi_m - \Phi_0}{m \cdot \beta} \quad (1)$$

From Eq. (1), the specific heat capacity can be easily calculated in accordance with the heat flux in the experimental DSC curve.

Normally, DSC spectra are analyzed at constant pressure, and because the nanocrystalline 3C-SiC particles used in this study are solid, the notion of constant pressure or volume is generally eliminated by a very small error. In this case, we can calculate the specific heat capacity from the DSC spectra as follow:

$$c = \frac{\Phi}{m \cdot \beta} \quad (2)$$

where,  $\Phi$  - is the heat flux in the DSC spectra,  $\beta$  - is the thermal processing rate,  $m$  - is the mass of the sample. The enthalpy and entropy of the system can be calculated in the given temperature range according to the calculated heat capacity by the following equations [12, 41]:

$$H = \int_0^T C dT \quad \text{and} \quad S = \int_0^T \frac{C}{T} dT \quad (3)$$

The free Gibbs energy of the system can be determined with a simple approach according to the calculated enthalpy and entropy values:

$$G = H - TS \quad (4)$$

In the present study, the specific heat capacity, free Gibbs energy, enthalpy, and entropy of nanocrystalline 3C-SiC particles were calculated at different temperatures using the equations (2), (3), and (4).

The analysis showed that 3C-SiC nanocrystals are extremely resistance materials to temperature. Nanocrystalline 3C-SiC particles have a very high melting point around 3103K. Therefore, 3C-SiC nanocrystals have extremely strong stability under heating up to 1200K. Simultaneously, HRTEM, SAED

and EDP analyzes showed that 3C-SiC nanocrystals do not undergo structural changes in extreme environments [25]. On the other hand, it has been noted that very small amounts of oxidation can occur on the surface of 3C-SiC nanocrystals at temperatures above about 1000K [12, 13].

Nanocrystalline 3C-SiC particles were investigated with the four different heating rates (5 K/min, 10 K/min, 15 K/min and 20 K/min) in the temperature range of 300 K – 1200 K. The heat capacity, Gibbs energy, enthalpy and entropy of nanocrystalline 3C-SiC particles at all thermal processing rates (5 K/min, 10 K/min, 15 K/min and 20 K/min) were calculated theoretically based on experimental results. Figure 1 briefly describes the spectra corresponding to 5 K/min and 20 K/min thermal processing rates. In the initial approach, as can be seen from the spectra, water or other additives adsorbed from the atmosphere are released from the system. Unlike conventional bulk materials, 3C-SiC crystals in nanoscale have an extremely large surface area and adsorption capacity. Previous experiments have shown that this feature is sharply distinguishes 3C-SiC nanocrystals from 3C-SiC wafer [42–45]. It is known that nanomaterials have a very large specific surface area (Specific Surface Area (SSA)) and these types of materials are surface active, which makes water or other compounds dependent on the nanoparticle surface immediately upon their contact with the atmosphere. Active surface is chemisorbed from the environment by weak interaction with H<sub>2</sub>O and OH groups. Linear increase in temperature breaks the weak reciprocal effect. From the observation of thermal curves, it can be concluded that as the temperature rises, the water or other impurities existed in the nanomaterial begin to leave the system. This process completed at about 450–500°C temperature. There is almost no change in the initial approach to the thermal spectra of nanocrystalline 3C-SiC particles from 500°C to 1000°C.

The temperature dependence of the specific heat capacity of nanocrystalline 3C-SiC particles at different thermal processing rates are given in Fig. 2. Specific heat capacity is proportional to the heating rate in the selected low temperature range (temperature range of 300 K – 350 K) (Fig. 2a). However, chaoticity is observed on the temperature dependence of the specific heat capacity in the wide temperature range (300K – 1200K) (Fig. 2b). The numerical value of the specific heat capacity is around the characteristic value ( $750 \text{ J}\cdot\text{kg}^{-1}\text{K}^{-1}$ ) for SiC in the low temperature region. However, there are sharp deviations with increasing temperature. Numerical value of the specific heat capacity is negative at  $T \geq 800\text{K}$  of temperature. This suggests that exothermic effects are observed in nanocrystalline 3C-SiC particles at temperatures  $\geq 800\text{K}$ . Thus, in this case, the temperature of the sample container in the experimental device is lower than the temperature of the sample. Moreover, the numerical value of the specific heat capacity is positive in the temperature range 300K-800K or corresponds to endothermic processes in the general approach.

The temperature dependences of the enthalpy of nanocrystalline 3C-SiC particles at different thermal processing rates are shown in Fig. 3. As can be seen from the figure, the numerical value of enthalpy decreases in the low temperature region in proportion to the thermal processing rate (Fig. 3a). The enthalpy of the system is chaotic, similar to the heat capacity at relatively high temperatures. However, in the general approach, the enthalpy of the system decreases with increasing thermal processing rate in the entire temperature range (Fig. 3b).

Based on the experimental results, the calculated entropy of the system for nanocrystalline 3C-SiC particles is shown in Fig. 4. As can be seen from the temperature dependences of the entropy of the system, in this case, according to the enthalpy and heat capacity, the entropy of the system decreases with increasing thermal processing rates in the low temperature range. The entropy of the system is a negative after the temperature is approximately  $T \geq 800\text{K}$ . This, in the general approach, can be explained by exothermic effects, similar to the specific heat capacity.

According to the experimental results, temperature dependences of the free Gibbs energy were calculated (Fig. 5). As can be seen from the figures, the numerical value of the free Gibbs energy is inversely proportional to the thermal processing rate (Fig. 5a). The numerical value of free Gibbs energy increases with increasing thermal processing rate, which is an indication that the system is more stable when heated at relatively low speeds. Obtained dependencies in a wide temperature range has shown that the numerical value of the free Gibbs energy increases almost in direct proportion to the temperature at relatively large temperature values. An increase in the numerical value of the free Gibbs energy for a system is, in a sense, an increase in the potential energy of the system (chemical potential). Any system tends to minimize its potential energy over time, and an increase in the value of free Gibbs energy in any system can reduce the stability of that system. Physically, this explains why the resistance of the system naturally decreases at high temperatures.

The numerical value of the free Gibbs energy calculated according to the experimental results is negative in the low temperature range. This means that the processes occurring in the system are spontaneous and the system can move towards equilibrium. Note that in the general approach at temperatures  $T < 800\text{K}$ , the numerical value of the free Gibbs energy varies around zero, which is an indication that the system is in equilibrium. Numerical value of the free Gibbs energy at temperatures  $T > 800\text{K}$  is positive. In this case, the processes in the system are not spontaneous, but changes can be observed in the opposite direction to the system. In the general approach, changes in temperature around  $740\text{K}$  can be explained to some extent by the Debye temperature [12, 46, 47]. However, more analytical investigations are needed to give an exact opinion.

## 4. Conclusion

Studies have shown that 3C-SiC nanocrystals exhibit extremely high surface activity. As a result of the extremely high surface activity of 3C-SiC nanoparticles, the hydroxyl or OH groups were observed to gather on the surface. It was found that the OH groups completely removed from the surface of 3C-SiC nanocrystals at the high temperatures. Groups O and H leave the surface of 3C-SiC nanocrystals in the temperature range of about  $467\text{-}755\text{K}$ , depending on the heating rate. At temperatures above  $755\text{K}$ , no traces of O and H groups are found on the surface of nanocrystalline 3C-SiC particles. It was observed that at relatively low heating rate of  $5\text{K}/\text{min}$ , the OH groups completely leave the nanomaterial surface at a temperature of about  $740\text{K}$ . However, the trace of hydroxyl groups have been determined between  $740\text{-}755\text{K}$  with the high heating rate (at  $20\text{K}/\text{min}$ ). Specific heat capacity of nanocrystalline 3C-SiC particles has been determined to be directly proportional to the heating rate in the low temperature range. Studies

have shown that the numerical value of the specific heat capacity varies around the value ( $750 \text{ J}\cdot\text{kg}^{-1}\text{K}^{-1}$ ) characteristic for 3C-SiC in the low temperature region. It was found that the numerical value of the specific heat capacity, enthalpy and entropy of the system are negative at relatively high temperatures, which was explained by the exothermic effects at the appropriate temperatures. According to the calculated free Gibbs energy, nanocrystalline 3C-SiC particles are found to be spontaneous or more stable at relatively low temperatures. Debye temperature was found to be around 740K for nanocrystalline 3C-SiC particles. It has been determined that the numerical value of free Gibbs energy increases with increasing thermal processing rate.

## References

1. Bukhari SZaighumA, Ha J-H (2017) Jongman Lee, In-Hyuck Song "Fabrication and optimization of a clay-bonded SiC flat tubular membrane support for microfiltration applications". *Ceram Int* 43/10:7736–7742
2. Meng, Zhang (2017) "Quasi-monodisperse  $\beta$ -SiC nanospheres: Synthesis and application in chemical-mechanical polishing". *J Phys Chem Solids* 103:1–5
3. Jia H, Luo Y, Zhang H, Xing D (2017) Peimiao Ma "A novel 4H-SiC MESFET with serpentine channel for high power and high frequency applications". *Superlattices Microstruct* 101:315–322
4. Gabriela Huminic A, Huminic C, Fleaca F, Dumitrache (2017) Ion Morjan "Thermo-physical properties of water based SiC nanofluids for heat transfer applications". *Int Commun Heat Mass Transfer* 84:94–101
5. Qian Xun B, Xun Z, Li P, Wang (2017) Zhiduan Cai "Application of SiC power electronic devices in secondary power source for aircraft". *Renew Sustain Energy Rev* 70:1336–1342
6. Ou X, Zhang X, Lowe T et al (2017) "X-ray micro computed tomography characterization of cellular SiC foams for their applications in chemical engineering". *Mater Charact* 123:20–28
7. Ralf Falgenhauer P, Rambacher L, Schlier et al (2017) "Electrically heated 3D-macro cellular SiC structures for ignition and combustion application". *Appl Therm Eng* 112:1557–1565
8. Kazuya Shimoda J-S, Park T, Hinoki (2007) Akira Kohyama "Influence of surface structure of SiC nano-sized powder analyzed by X-ray photoelectron spectroscopy on basic powder characteristics". *Appl Surf Sci* 253/24:9450–9456
9. Kim K-S (2009) Gwiy-Sang Chung "Growth and characteristics of polycrystalline 3C-SiC films for extreme environment micro/nano-electromechanical systems. *Sensors Actuators A: Physical* 155/1:125–130
10. Arab Juneghani M, Farzam M (2013) H. Zohdirad "Wear and corrosion resistance and electroplating characteristics of electrodeposited Cr-SiC nano-composite coatings. *Transactions of Nonferrous Metals Society of China* 23/7:1993–2001
11. Shen MJ, Wang XJ, Ying T, Wu K (2016) W.J. Song "Characteristics and mechanical properties of magnesium matrix composites reinforced with micron/submicron/nano SiC particles". *J Alloy*

12. Elchin M, Huseynov TG, Naghiyev, Ulviyya S (2020) Aliyeva "Thermal parameters investigation of neutron-irradiated nanocrystalline silicon carbide (3C-SiC) using DTA, TGA and DTG methods". *Physica B* 577:411788
13. Elchin M (2020) Huseynov "Thermal stability and heat flux investigation of neutron-irradiated nanocrystalline silicon carbide (3C-SiC) using DSC spectroscopy". *Ceram Int* 46/5:5645–5648
14. Elchin M. Huseynov, Tural G (2021) Naghiyev "Study of thermal parameters of nanocrystalline silicon carbide (3C-SiC) using DSC spectroscopy". *Applied Physics A* volume 127:267
15. Elchin Huseynov, Adil Garibov " Effects of neutron flux on the temperature dependency of permittivity of 3C-SiC nanoparticles" *Silicon* 9/5, 753–759, 2017
16. Elchin Huseynov, Anze Jazbec "EPR spectroscopic studies of neutron-irradiated nanocrystalline silicon carbide (3C-SiC)" *Silicon* 11/4, 1801–1807, 2019
17. Huseynov EM, Naghiyev TG (2019) N.R. Abbasov "Radioactivity study of 3C-SiC nanoparticles under the neutron flux at the TRIGA Mark II type research reactor". *Advanced Physical Research* 1(1):42–51
18. Elchin MHuseynov, Tural GNaghiyev, Adil AGaribov et al. "EPR spectroscopy of neutron irradiated nanocrystalline boron nitride (h-BN) particles" *Ceramics International*, <https://doi.org/10.1016/j.ceramint.2020.11.075>
19. Elchin M (2018) Huseynov "Neutron irradiation, amorphous transformation and agglomeration effects on the permittivity of nanocrystalline silicon carbide (3C-SiC)". *NANO* 13/3:1830002
20. Elchin M (2018) Huseynov "Dielectric loss of neutron-irradiated nanocrystalline silicon carbide (3C-SiC) as a function of frequency and temperature". *Solid State Sci* 84:44–50
21. Elchin M (2018) Huseynov "Current-voltage characteristics of neutron irradiated nanocrystalline silicon carbide (3CSiC)". *Physica B* 544:23–27
22. Elchin M. Huseynov "Neutron irradiation effects on the temperature dependencies of electrical conductivity of silicon carbide (3C-SiC) nanoparticles" *Silicon* 10/3, 995–1001, 2018
23. Elchin M. Huseynov "Permittivity-frequency dependencies study of neutron-irradiated nanocrystalline silicon carbide (3C-SiC)" *NANO* 12, No. 6, 1750068, 2017
24. Elchin, Huseynov et al (2016) "Effects of neutron flux on the nano silica particles: ESR study". *Mod Phys Lett B* 30/8:1650115
25. Elchin M (2017) Huseynov "Investigation of the agglomeration and amorphous transformation effects of neutron irradiation on the nanocrystalline silicon carbide (3C-SiC) using TEM and SEM methods". *Physica B* 510:99–103
26. Naghiyev TG (2020) Computer simulation of (n, p) modifications in silicon nitride (Si<sub>3</sub>N<sub>4</sub>) nanoparticles. *Int J Mod Phys B* 34(32):2050318
27. T.G. Naghiyev "Computer modeling for the study of (n, p) and (n, α) modifications in AlN nanoparticles" *Journal of the Korean Physical Society* 78, 232–235, 2021

28. T.G. Naghiyev "An investigation of silicon nitride (Si<sub>3</sub>N<sub>4</sub>) nanoparticles interaction with neutrons" *Modern Physics Letters B* 35/06, 2150104, 2021
29. Elchin, Huseynov et al (2018) "Fourier transform infrared spectroscopic study of gamma irradiated SiO<sub>2</sub> nanoparticles". *Int J Mod Phys B* 32/7:1850074
30. Yang CC (2014) Yiu-Wing Mai "Thermodynamics at the nanoscale: A new approach to the investigation of unique physicochemical properties of nanomaterials". *Materials Science Engineering R* 79:1–40
31. Hartmann M (2005) Günter Mahler, Ortwin Hess "Nano-thermodynamics: On the minimal length scale for the existence of temperature". *Physica E* 29(1–2):66–73
32. Ralph VC (2003) "Critical behavior from Landau theory in nanothermodynamic equilibrium". *Phys Lett A* 315:3–4 / ) 313–318
33. Vladimir García-Morales, Cervera J, Julio Pellicer "Correct thermodynamic forces in Tsallis thermodynamics: connection with Hill nanothermodynamics" *Phys Lett A* 336/1 (2005) 82–88
34. J.Sunilv et al. "The thermal properties of CaO-Nanofluids" *Vacuum* 161, 2019, 383–388
35. Israel, López-Báez et al. "Surface oxidation of Ni<sub>20</sub>Cr/Cr<sub>30</sub>2 composite processed by ball milling and HVOF thermal spraying" *Vacuum* 144, 2017, 27–35
36. Yueting, Wang et al. "Experimental and numerical investigations of the effect of charge density and scale on the heat transfer behavior of Al/CuO nano-thermite" *Vacuum* 184, 2021, 109878
37. Jing, Wang et al. "A vacuum calcination route to high-surface-area MgO nanoplates for superior arsenate adsorption and catalytic properties" *Vacuum* 158, 2018, 231–235
38. Matlab N. Mirzayev "Simultaneous measurements of heat flow rate and thermal properties of nano boron trioxide under neutron irradiation at the low and high temperature" *Vacuum* 173, 2020, 109162
39. Ricardo D. Brancher et al. "A kinetic model for gas adsorption-desorption at solid surfaces under non-equilibrium conditions" *Vacuum* 174, 2020, 109166
40. Hohne GWH. Hemminger WF (2003) H.-J. Flammersheim "Differential Scanning Calorimetry". Springer-Verlag Berlin Heidelberg 298:34–42
41. C. Schick "Differential scanning calorimetry (DSC) of semicrystalline polymers" *Anal Bioanal Chem* 395 (2009) 1589–1611
42. Mojmír M et al (2019) "X-ray diffraction on stacking faults in 3C-SiC epitaxial microcrystals grown on patterned Si(0 0 1) wafers". *J Cryst Growth* 507:70–76
43. Polychroniadis E et al (2004) Microstructural characterization of very thick freestanding 3C-SiC wafers. *J Cryst Growth* 263:68–75
44. Chung G-S (2005) Roya Maboudian "Bonding characteristics of 3C-SiC wafers with hydrofluoric acid for high-temperature MEMS applications". *Sensors Actuators A: Physical* 119:599–604
45. Chaussende D et al (2008) "Prospects for 3C-SiC bulk crystal growth". *J Cryst Growth* 310:976–981
46. Thakore BY, Khambholja SG, Vahora AY (2013) N. K. Bhatt and A. R. Jani "Thermodynamic properties of 3C–SiC". *Chin Phys B* 22:106401

## Figures

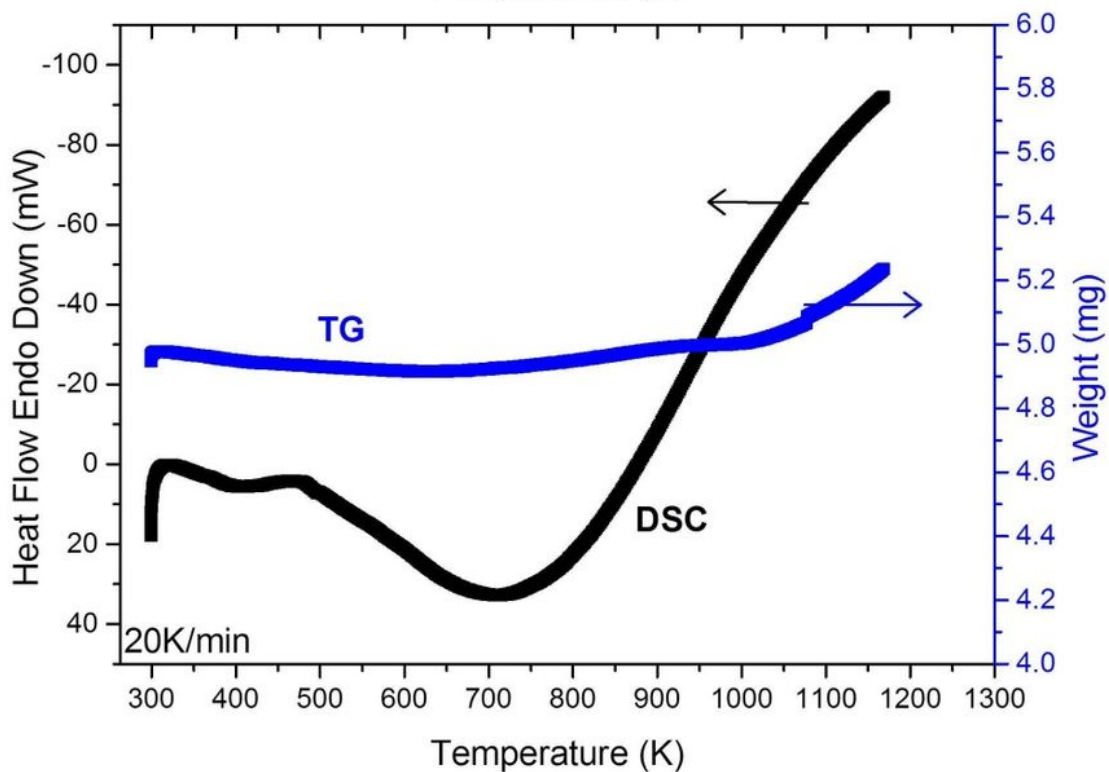
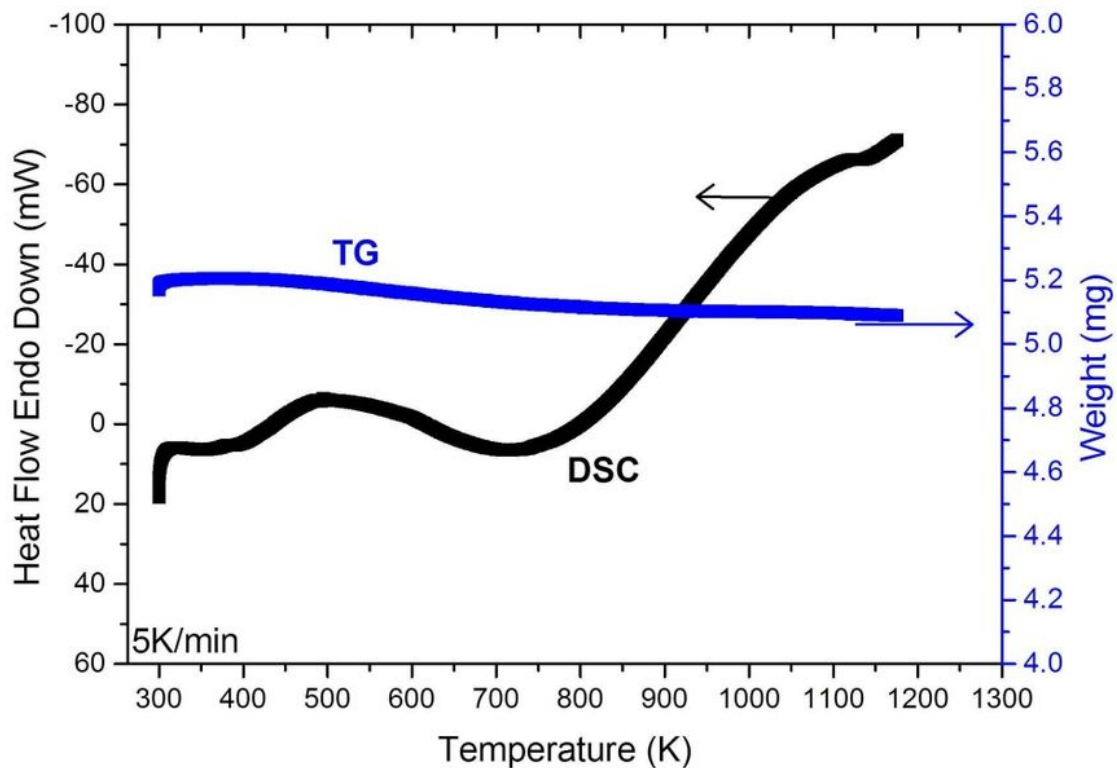


Figure 1

DSC and TG spectra at different thermal processing rates of nanocrystalline 3C-SiC particles.

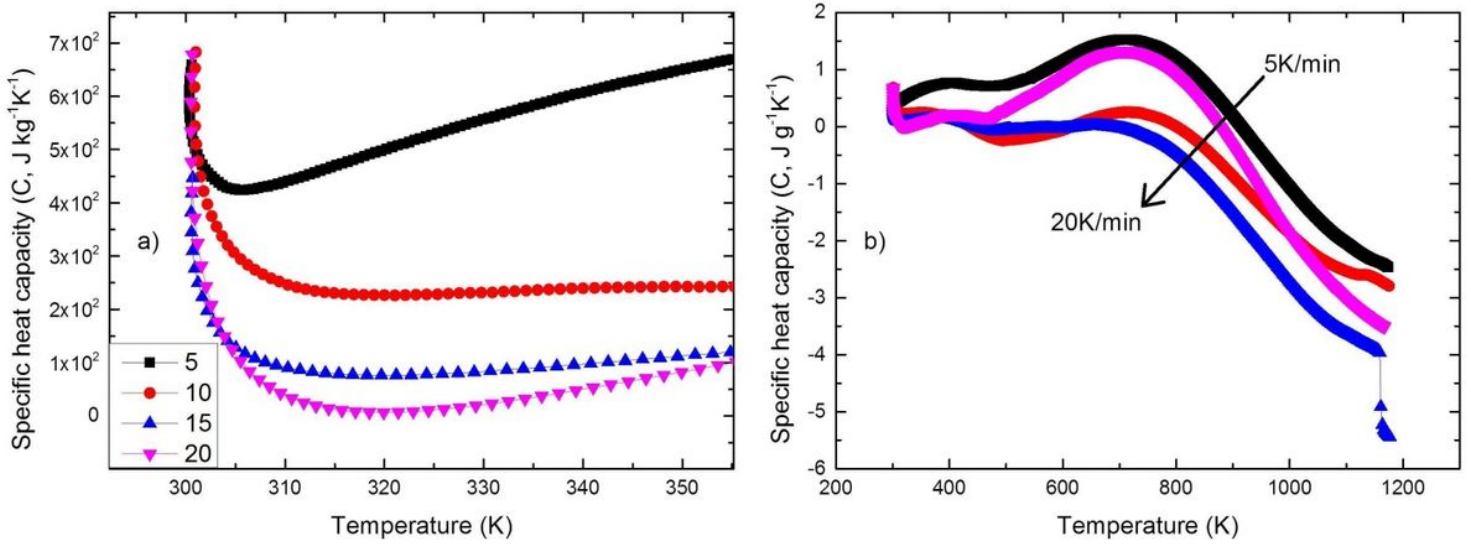


Figure 2

Temperature dependences of specific heat capacity at different thermal processing rates of nanocrystalline 3C-SiC particles (a - in a selected range, b - in a wide range).

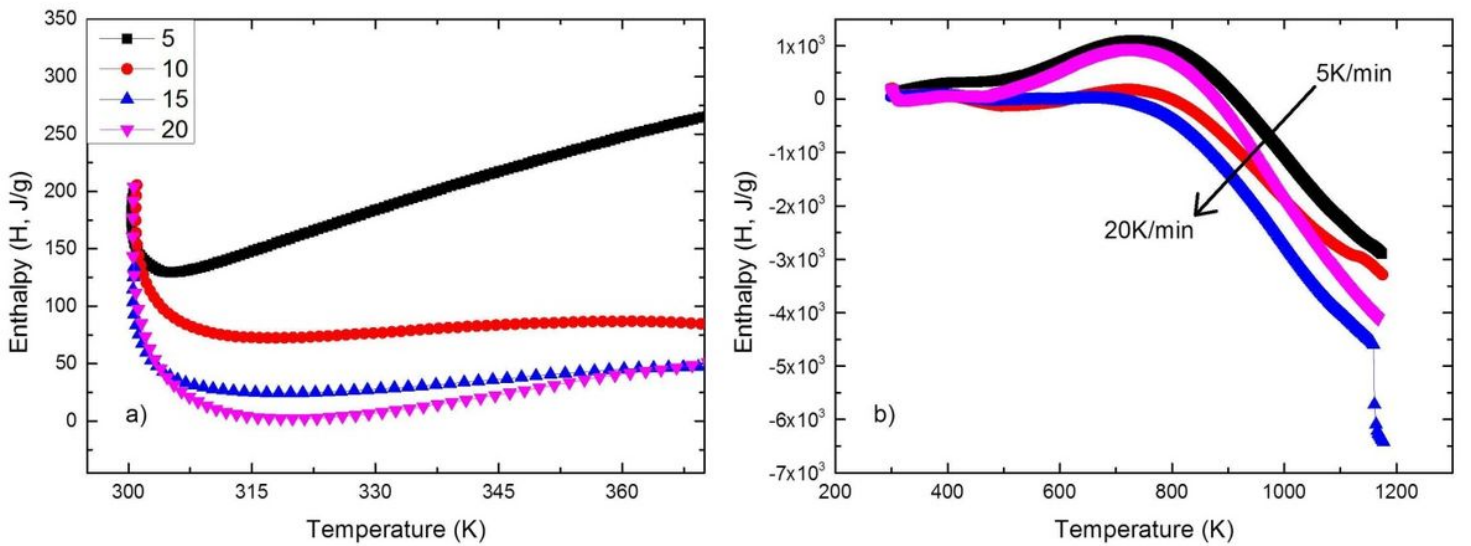
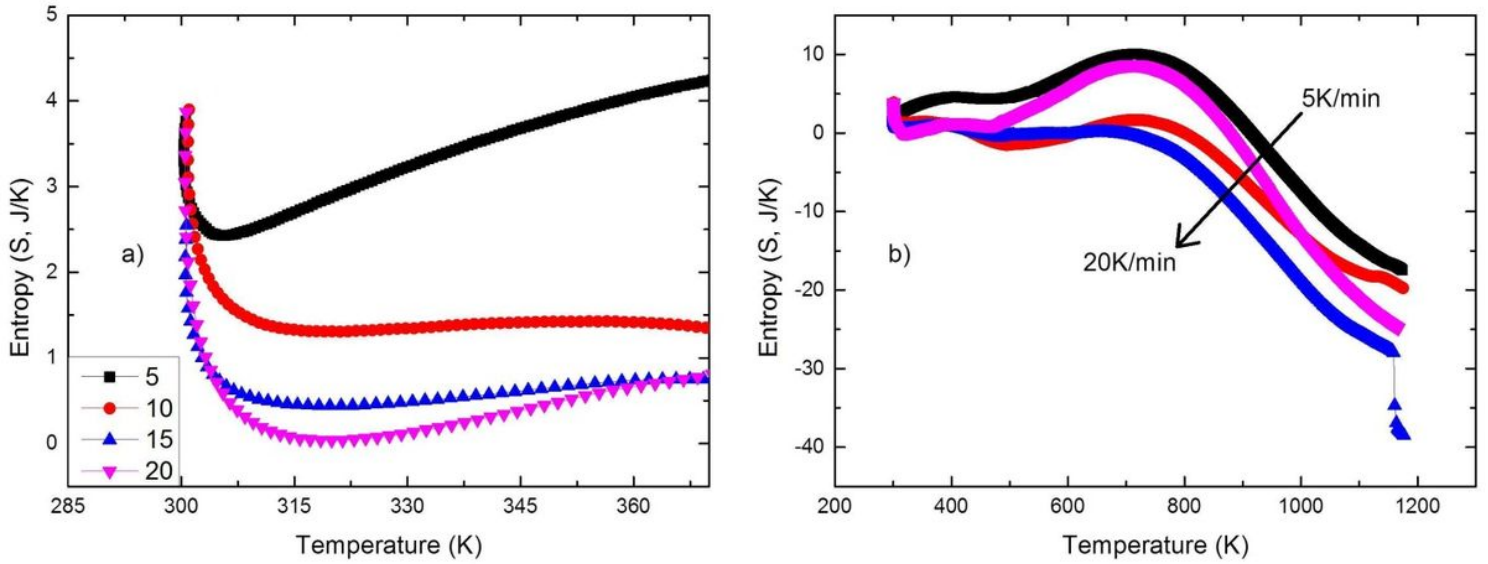


Figure 3

Temperature dependences of enthalpy of nanocrystalline 3C-SiC particles at different thermal processing rates (a - in a selected range, b - in a wide range).



**Figure 4**

Temperature dependences of entropy of nanocrystalline 3C-SiC particles at different thermal processing rates (a - in a selected range, b - in a wide range).

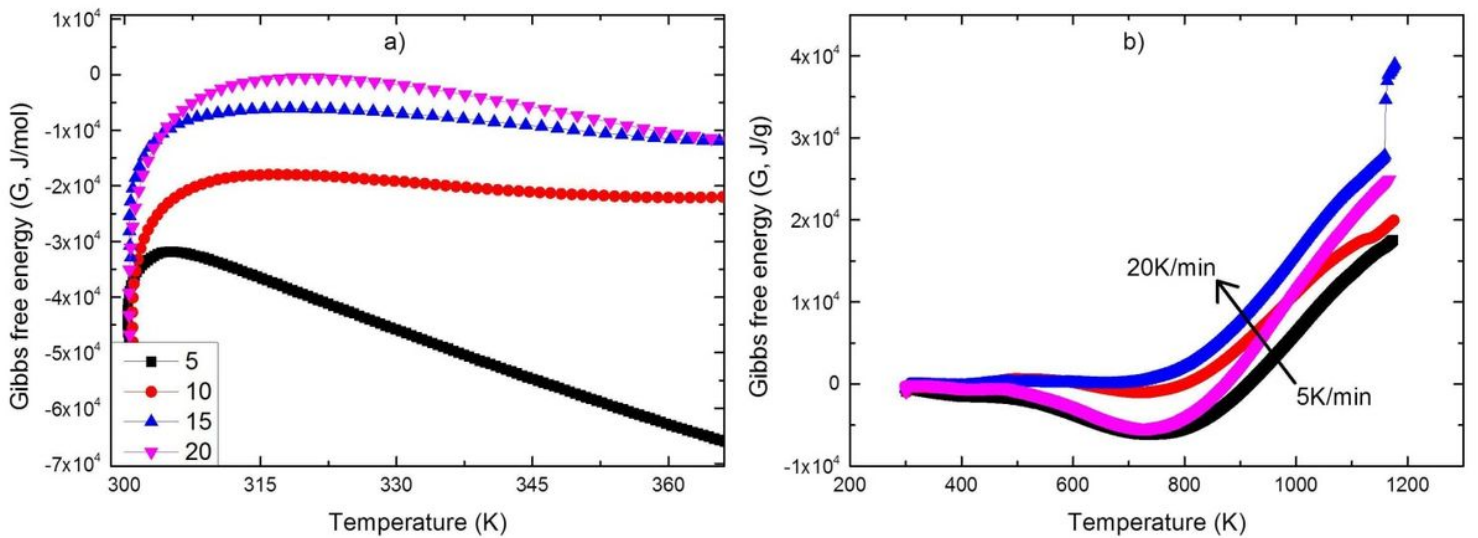


**Figure 5**

Temperature dependences of free Gibbs energy at different thermal processing rates of nanocrystalline 3C-SiC particles (a - in a selected range, b - in a wide range).